UC Irvine
UCI Open Access Publishing Fund

Title
Shrink-Induced Silica Structures for Far-field Fluorescence Enhancements

Permalink
https://escholarship.org/uc/item/1xn7v1pb

Journal
Advanced Optical Materials, 1(8)

ISSN
2195-1071

Authors
Lin, Sophia
Sharma, Himanshu
Khine, Michelle

Publication Date
2013-08-01

DOI
10.1002/adom.201300180

Supplemental Material
https://escholarship.org/uc/item/1xn7v1pb#supplemental

Copyright Information

Peer reviewed

ADVANCED
OPTICAL
MATERIALS

www.advopticalmat.de

Materials Views

www.MaterialsViews.com

FULL PAPER

Shrink-Induced Silica Structures for Far-field Fluorescence Enhancements

Sophia Lin, Himanshu Sharma, and Michelle Khine*

Dense multiscale silica (SiO$_2$) micro- and nanostructures are fabricated on a pre-stressed polymer film. This novel SiO$_2$ substrate serves as a robust platform to enhance the fluorescence signal of bound biomolecules. Through a combination of surface concentration, light scattering, and changes in the photophysical properties of the confined dye molecules, dramatic fluorescence signal enhancements (average = 116 times greater than on planar glass) and increased signal-to-noise ratio (76:1) are demonstrated with tetramethylrhodamine isothiocyanate (TRITC)-conjugated streptavidin (STRITC) on SiO$_2$ structures. Enhanced detection sensitivity of STRITC over glass on the SiO$_2$ structures is achieved down to a detection limit of 11 ng mL^{-1}. Such significant fluorescence signal enhancements have importance in practical applications such disease diagnostics and surface sensing.

1. Introduction

Fluorescence is widely used for chemical sensing, biomolecule detection, disease diagnostics, and various applications in biology. Ongoing challenges persist in improving detection sensitivity and the signal-to-noise ratio (SNR) of low-abundance target molecules. Efforts to improve detection sensitivity and robustness of fluorescent assays have resulted in the development of brighter and more photostable fluorescent labels,[1,2] advancements of traditional imaging devices and techniques,[3] and engineered surface structures for signal enhancement.[4–6]

Examples of effective surface structures for fluorescence signal enhancement include metal nanostructures and nanoparticles that couple excitation with surface plasmons and photonic crystals that act as optical resonators.[7–9] These structures typically use expensive materials such as gold and silver, require extensive fabrication steps for precise control of homogeneous or periodic surface features, and necessitate specialized equipment (e.g. 2-photon microscopy). Importantly, while large fluorescence enhancements have been observed, such plasmon-coupled effects suffer from practical limitations including: localized near-field effects with enhancements occurring only within nanometric lengths from the surface, heterogeneous enhancements with small areas of 'hot spots', and enhancements which are wavelength dependent. Such practical drawbacks impede progress in translating these large enhancements into solutions for deployable robust detection.

It has recently been observed that enhancements of fluorescent properties can be achieved through covalent encapsulation of dye into SiO$_2$-based nanoparticles.[10–13] Studies of dye-encapsulated SiO$_2$ nanoparticles have suggested that these photophysical changes are dependent on internal architecture of the SiO$_2$ structures.[14] Immobilization of the fluorescent dye within the SiO$_2$ core–shell is suggested to restrict molecular mobility, which can lead to reduced nonradiative relaxation and subsequently increased quantum yield.[15,16] SiO$_2$ encapsulation has also been reported to result in enhancement of radiative decay rate due to the difference between the refractive indices of rhodamine dyes and SiO$_2$ surroundings.[15–17]

Leveraging these properties, as well as the mechanical stability and chemical versatility of SiO$_2$, we develop a strategy to create a robust and scalable fluorescence enhancing platform based on low-cost commodity shrink wrap film. We have previously shown that we are able to achieve concentration of adsorbed molecules by leveraging the heat-induced retraction properties of polyolefin (PO) sheets.[18] We have also shown that the deposition of a stiff, non-shrinkable material such as metal onto the PO film results in buckling when the substrate is heated.[19] Here, we demonstrate that this strategy is extensible for SiO$_2$. We use the biotin-streptavidin hybridization as it is a versatile binding system that has been shown to form the basis of many detection methods, including DNA, protein, and aptamer sensing.[20–24] We predict that by covalently linking the biomolecules onto the shrinkable SiO$_2$ substrate: (1) the fluorophores are brought closer in proximity to each other which results in signal concentration, (2) the SiO$_2$ structures create a highly porous surface that results in light scattering, and (3) the covalent attachment of fluorophore within the SiO$_2$ structures causes changes in the photophysical properties of the dye. Together, this results in both dramatic increases in the signal intensity and fluorescence enhancement factor. To understand the mechanisms of such enhancements, we characterize our SiO$_2$ structures, demonstrate fluorescence signal enhancements, investigate the effects of dye–silica interaction on absorption, emission, and look into the detection sensitivity of the substrate.

S. Lin, H. Sharma, Prof. M. Khine
Department of Chemical Engineering
and Materials Science
University of California
Irvine (UCI), Irvine, CA 92697, USA
Prof. M. Khine
Department of Biomedical Engineering
University of California
Irvine (UCI), Irvine, CA 92697, USA
E-mail: mkhine@uci.edu

www.MaterialsViews.com
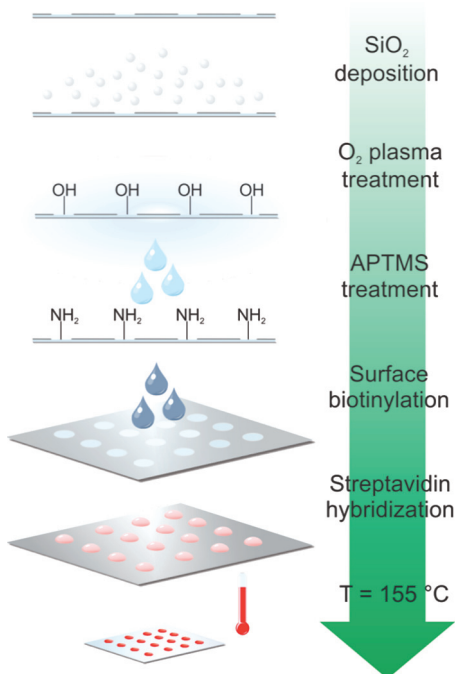
ADVANCED
OPTICAL
MATERIALS
www.advopticalmat.de

FULL PAPER

Figure 1. Schematic illustrating the fabrication of a fluorescence enhancing PO–SiO$_2$ substrate. Clean PO is coated with a thin layer of SiO$_2$ through ion-beam sputter deposition, treated with O$_2$ plasma, and reacted with APTMS for the formation of reactive primary amines. The silanized surface was linked with biotin, reacted with STRITC, and shrunk.

2. Results and Discussion

2.1. Preparation of PO–SiO$_2$ Substrate and Biomolecule Attachment

We leverage the stiffness mismatch between the thin SiO$_2$ layer and the PO film to create SiO$_2$ micro- and nanostructures. The multi-scale substrate that results in enhanced fluorescence signal is prepared following the procedure illustrated in **Figure 1**. Briefly, a home-made shadow mask was applied to a clean PO surface prior to sputter deposition of SiO$_2$ to form PO–SiO$_2$ substrates. The surfaces were chemically activated through O$_2$ plasma treatment and then functionalized with primary amine groups for further biomolecule attachment. The PO–SiO$_2$ surfaces were biotinylated and then hybridized with a STRITC (here on referred to as PO–SiO$_2$–STRITC). Substrates were heated at $T = 155$ °C, which induces retraction of the substrate and causes the SiO$_2$ thin film to buckle and crack.

Figure 2a,b are top down SEM images of the shrunk PO–SiO$_2$ substrate. The SEM image illustrates the formation of a continuous population of heterogeneous surface structures. The cross section SEM image (Figure 2c) demonstrates integration of the SiO$_2$ layer with the PO film that occurs when the PO film is heated above its glass transition temperature. Integration of the SiO$_2$ into the PO film is also supported from energy-dispersive X-ray spectroscopy (EDS) data (Figure S1). The SiO$_2$ structures are patterned into distinct islands by applying a shadow mask prior to SiO$_2$ deposition (Figure 2d).
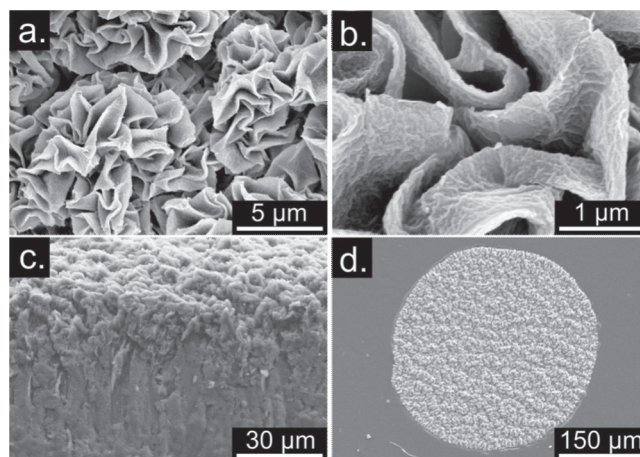

Figure 2. SEM images of the PO–SiO$_2$ substrate. Top down SEM images of shrunk PO–SiO$_2$ substrate showing micro- and nanostructures at different magnifications (a,b) and a cross section SEM image of the PO–SiO$_2$ substrate (c). The PO film can be patterned to form discrete SiO$_2$ islands (d).

2.2. Optical Characterization

To examine the effects of the SiO$_2$ structures on the photophysical properties of the linked fluorescent dye, optical properties of the reacted substrate and controls were measured. The UV-Vis absorption spectra of STRITC, glass-STRITC (STRITC bound to glass), and shrunk PO-SiO$_2$-STRITC are shown in **Figure 3**a. STRITC exhibits two absorption maxima at 520 and 549 nm attributed to the presence of dimeric and monomeric species reported to occur for rhodamine dyes at high concentrations ($A_{520/549} = 0.89$).[25] Glass-STRITC also exhibits an absorption maximum at 549 nm. Covalent linkage of STRITC within the SiO$_2$ structures is not observed to cause spectral shifts in peak absorbance. The absorption spectra of the shrunk PO-SiO$_2$-STRITC substrate shows higher optical density at higher energies, which fits well to Rayleigh scattering, suggesting that shrinking of the PO-SiO$_2$ substrate creates rough porous structures with small surface features that together result in light scattering.[26,27]

The emission spectra are shown in Figure 3b. The emission intensity maximum for the STRITC occurs at 575 nm. While covalent attachment of the STRITC on glass does not cause a change in the absorption wavelength, it is observed to cause a slight red shift of 3.0 nm for the emission wavelength for STRITC on the PO–SiO$_2$ substrate. This slight red shift in emission wavelength can be attributed to the change in molecular surrounding experienced by the STRITC dye since it is known that dye molecules are affected by microenvironment polarity.[28] However, the observed spectral shifts are insignificant and it can be suggested that confinement of the dye molecules within the SiO$_2$ structures does not result in changes of the dye's electronic structure.

2.3. Fluorescence Signal Enhancement on PO–SiO$_2$ Substrate

Fluorescence signal enhancement on PO–SiO$_2$ substrates were investigated using the model biotin-streptavidin binding

a.

b.

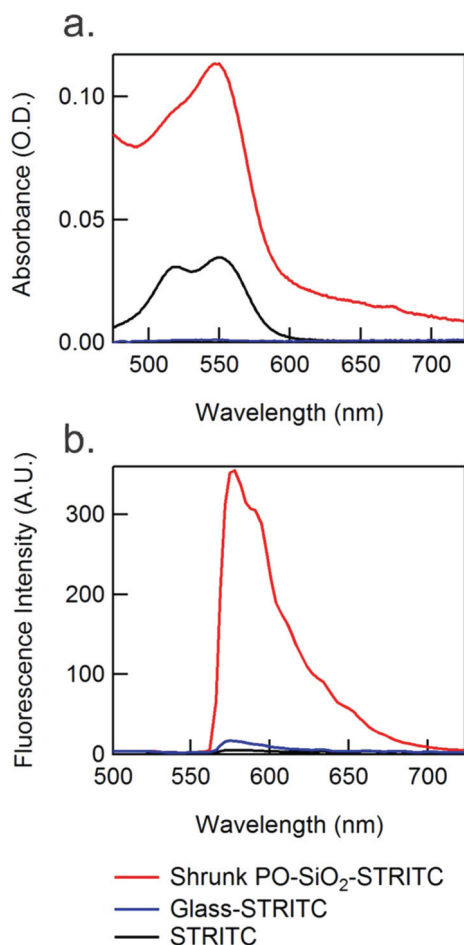— Shrunk PO-SiO₂-STRITC
— Glass-STRITC
— STRITC

Figure 3. Absorption spectra of STRITC free dye, glass–STRITC, and PO–SiO₂–STRITC (a). Emission spectra of STRITC free dye, glass–STRITC, and PO–SiO₂–STRITC (b).

system. Substrates were prepared as described above and shrunk thermally. The fluorescence images of the patterned substrates following shrinkage are shown in **Figure 4**a. The 3D intensity distribution profiles (Figure 4b) illustrate fluorescence uniformity over the SiO₂ islands on the shrunk PO–SiO₂–STRITC substrates and that enhanced fluorescence signal is not localized to nanometric hotspots. The increase in fluorescence signal is assessed and results are compared to that obtained on glass–STRITC and thermally shrunk PO (PO–STRITC). The average fluorescence signal increase (SI) of the substrate is calculated to be the fluorescence signal obtained after shrinking minus the background (here defined as the substrate without the presence of dye), over the fluorescence signal before shrinking minus the background:

$$SI = \frac{Intensity_{postshrunk} - Intensity_{postshrunk,bg}}{Intensity_{preshrunk} - Intensity_{preshrunk,bg}} \tag{1}$$

As previously reported, the PO film experiences a 77% reduction in each length upon heating, which results in a theoretical 20-fold consolidation of surface area.[18] The PO–STRITC experiences a fluorescence SI of 14-fold (standard error (SE) = 0.57) due to concentration of the surface bound fluorophores. This slight decrease in experimental value compared to the theoretical expectation is attributed to concentration quenching effect from bringing the fluorescent molecules close in proximity. Interestingly, an approximate 50-fold (SE = 1.9) fluorescence SI is observed on the shrunk PO–SiO₂–STRITC substrates. Notably, the fluorescence SI is accompanied with a significantly increased SNR (defined as the ratio of the raw fluorescence signal to the background signal) from 11:1 to 76:1. The increased fluorescence intensity from shrinking the PO–SiO₂–STRITC substrate exceeds that observed from just concentrating the fluorescent molecules (as seen on the PO–STRITC substrate). This suggests that the additional increase of fluorescence signal on the PO–SiO₂–STRITC substrate is

a.

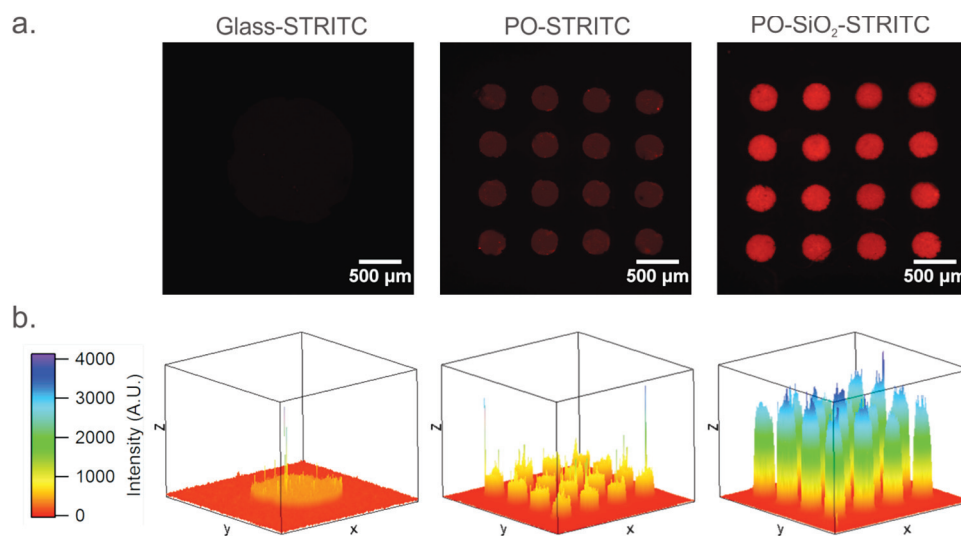Glass-STRITC   PO-STRITC   PO-SiO₂-STRITC

b.

Figure 4. Fluorescent images of the patterned substrates for heated glass, thermally shrunk PO, and thermally shrunk PO–SiO₂ bound with biotin and STRITC (a) and the corresponding 3D fluorescence intensity profiles (b).

www.MaterialsViews.com

ADVANCED
OPTICAL
MATERIALS
www.advopticalmat.de

FULL PAPER

due to presence of SiO$_2$ structures and not from bringing the fluorophores into close proximity of each other. We also show on the glass surface that the application of heat does not cause signal amplification or significant signal degradation (SI, glass = 0.92, SE = 0.019) and that the SNR does not change considerably (from 5.7:1 to 5.2:1 following heating). Therefore the observed increase in fluorescence intensity on the shrunk PO–STRITC and the shrunk PO–SiO$_2$–STRITC cannot be attributed to changes in the fluorophore due to heating.

For comparison between substrates, the average fluorescence enhancement factors (EFs) are calculated. The fluorescence EF is defined to be the fluorescence intensity of substrate minus the background over the fluorescence intensity of the comparison substrate minus its respective background:

$$EF = \frac{Intensity_{exp,postshrunk} - Intensity_{exp,bg}}{Intensity_{control,postshrunk} - Intensity_{control,bg}} \quad (2)$$

Compared to the glass–STRITC, the shrunk PO–SiO$_2$–STRITC substrate has an average fluorescence EF of 116 (SE = 9.7). We observe a higher fluorescence signal on the flat PO–SiO$_2$–STRITC relative to glass–STRITC, and we attribute the higher signal to the increased surface area that forms during the sputter deposition of SiO$_2$. Increased surface area subsequently allows for an increased number of binding sites for biomolecule attachment. To distinguish between concentrating surface biomolecules and additional effects from the SiO$_2$ structures, the EF of the shrunk PO–SiO$_2$–STRITC substrate over the shrunk PO–STRITC is evaluated. Experimental results suggest that the SiO$_2$ structures contributes in an additional 5.0-fold enhancement (SE = 0.74) of fluorescence signal on top of the concentrating effects.

2.3.1. Binding Study with Alternate Dye

While fluorescence enhancements that arise from plasmon resonances are highly dependent on nanostructure size and shape,[29] we show that increased fluorescence signal and fluorescence enhancement factors on our PO–SiO$_2$ substrates are not restricted to a particular wavelength or structure size. 10 µg mL^{-1} Cy2-conjugated streptavidin were spotted onto unshrunk biotinylated substrates as previously performed. Upon shrinking the substrate, a 39-fold (SE = 1.6) and 11-fold (SE = 1.2) increase in the fluorescence signal is observed on the shrunk PO–SiO$_2$ substrate and the shrunk PO substrate, respectively. The increases in fluorescence signal correspond to averaged enhancement factors of 106 (SE = 9.5) and 5.0 (SE = 0.27) for the shrunk PO–SiO$_2$ relative to the heated glass and shrunk PO substrate. An increase in SNR is also experienced on the shrunk PO–SiO$_2$ substrate from 13:1 to 29:1.

2.4. Lower Limits of Detection

To evaluate detection sensitivity of the PO–SiO$_2$ substrates, a concentration curve of STRITC was performed on the PO–SiO$_2$ and glass substrate. We use the biotin-streptavidin hybridization since this system can be applied towards real immunoassays through DNA, protein, or aptamer linking. The results are plotted in **Figure 5**. The fluorescence signal corresponding to the limit of
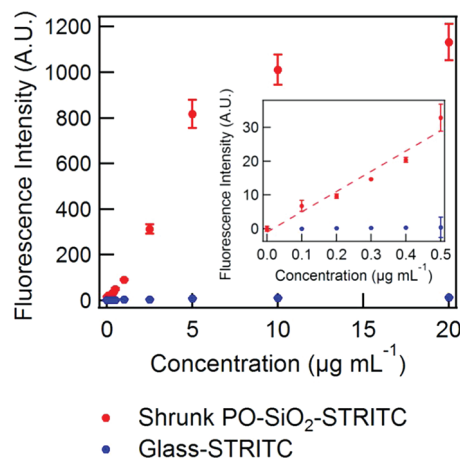
Figure 5. A plot of the fluorescence intensity as a function of STRITC concentration on the shrunk PO–SiO$_2$ substrate and the glass surface. The inset graph is a zoom of the lower STRITC concentrations, background subtracted for each respective substrate.

detection (LOD) is defined to be the mean of the background plus three times the standard deviation of the background. The LOD is calculated to be 0.26 µg mL^{-1} (SE = 0.026) on the heated glass surface. In contrast, the shrunk PO–SiO$_2$ substrate is able to yield a lower LOD of 11 ng mL^{-1} (SE = 0.0027). This proof-of-concept demonstrates that the PO–SiO$_2$ substrate has higher detection sensitivity relative to planar glass surface. This ability to reach lower limits of detection suggests the possibility for applications in disease diagnostics and point-of-care testing.

3. Conclusion

In this work, we have presented a rapid method to create SiO$_2$ micro- and nanostructures, demonstrated the ability of our structures to enhance fluorescence signal of bound fluorophores, and achieved lower limits of detection on the PO–SiO$_2$ substrates. We also investigated the photophysical properties of the dye on the SiO$_2$ structures. Fabrication of SiO$_2$ structures is simple and rapid, leading to signal enhancement within minutes. Structures are directly integrated on chip and defined regions of SiO$_2$ structures are easily established. The observed far-field fluorescence enhancements on our structures are robust and highly reproducible.

Due to the well-established conjugation chemistries and high biocompatibility of SiO$_2$, our PO–SiO$_2$ substrate has applications in surface sensing technologies. Integration of our SiO$_2$ structures into microfluidic devices for point-of-care applications is readily realized as similar structures have been demonstrated to be robustly integrated into the plastic used for microfluidic chips.[30]

4. Experimental Section

Fabrication of Functionalized PO–SiO$_2$ Substrate: PO film (955-D, Sealed Air Corporation) was cleaned in isopropyl alcohol (IPA) and double deionized water (ddH$_2$O) and dried with pressurized air. To

pattern discrete regions of SiO$_2$, a sealing tape mask (Nunc) was applied to the clean PO film surface prior to SiO$_2$ deposition. A mask composed of a four-by-four array of circles with radii of 7.0 µm was designed using automated Computer-Aided-Design (AutoCAD) software and cut with a VersaLASER cutter. Following application of the sealing tape mask, the PO surface was then coated with SiO$_2$ using an ion-beam sputter coater at deposition time of 20 min (MODEL IBS/e, South Bay Technology, Inc.). The SiO$_2$-modified PO substrates (PO–SiO$_2$) were treated with oxygen plasma (Plasma Prep II, SPI supplies) for 5 min and then immersed into a solution of 3-(aminopropyl)trimethoxysilane (APTMS) in ethanol (2% v/v) for 45 min at room temperature. The samples were rinsed with ethanol and ddH$_2$O, dried with pressurized air, and cured overnight in ambient conditions. Amine-functionalized PO–SiO$_2$ substrates were used immediately after preparation.

Binding Study: A model immunoassay was performed by reacting silanized PO–SiO$_2$ surfaces with EZ-Link Sulfo-NHS-LC-biotin (0.10 mg mL^{-1}) (Piercenet Thermoscientific) for 1 h at room temperature. The surfaces were washed, dried with pressurized air, and spotted with tetramethylrhodamine isothiocyanate (TRITC)-conjugated streptavidin (10 µg mL^{-1}) (Jackson ImmunoResearch Inc.). Substrates were incubated in a humidified chamber for 1 h before washing and drying, and shrunk by applying heat at 155 °C for 3 min. Fluorescent images were taken using a custom built upright fluorescence microscope (Olympus) using a 2x objective (NA = 0.055, Edmond Optics) and analyzed using ImageJ.

Characterization of SiO$_2$ Substrates: Shrunk PO–SiO$_2$ surface structures were characterized using scanning electron microscopy (SEM). Shrunk PO–SiO$_2$ substrates were sputter coated with 7.0 nm gold (Q150R S, Quorum Technologies) and SEM images were obtained with 10 kV beam and 12 mm working distance (Hitachi S-4700-2 FE-SEM Scanning Electron Microscope). Energy-dispersive X-ray spectroscopy (EDS) of substrate composition was performed on shrunk PO–SiO$_2$ sputtered with 7.0 nm gold and obtained with a 10 kV beam and 12 mm working distance (Philips XL-30 FEG Scanning Electron Microscope).

Optical Properties: UV-visible absorption spectra were collected using a PerkinElmer Lambda 950 UV/Vis/NIR Spectrophotometer with the help of the Law group. For highly scattering surfaces, a 60 mm integrating sphere was used. Fluorescence spectra were measured with an excitation wavelength of 561 nm and emission was collected from 416–728 nm (Zeiss LSM 710) using a 20x objective (NA = 0.4, Zeiss Korr C-Apochromat) and an argon laser.

Lower Limits of Detection: PO–SiO$_2$ and glass substrates were biotinylated as previously described. Surfaces were spotted with stock concentrations of STRITC (20, 10, 5, 2.5, 1.0, 0.50, 0.40, 0.30, 0.20, 0.10, and 0.0 µg mL^{-1}) and incubated per conditions described above. Following heating at $T = 155$ °C, samples were imaged as previously described.

Supporting Information

Supporting Information is available from the Wiley Online Library or from the author.

Acknowledgements

[1] N. P. Voloshina, R. P. Haugland, J. Bishop, M. Bhalgat, P. Millard, F. Mao, W. Y. Leung, R. P. Haugland, *Mol. Biol. Cell* **1997**, *8*, 2017–2017.

[2] R. B. Altman, D. S. Terry, Z. Zhou, Q. S. Zheng, P. Geggier, R. A. Kolster, Y. F. Zhao, J. A. Javitch, J. D. Warren, S. C. Blanchard, *Nat. Methods* **2012**, *9*, 68–U178.

[3] H. R. Petty, *Microsc. Res. Techniq.* **2007**, *70*, 687–709.

[4] E. D. Diebold, N. H. Mack, S. K. Doom, E. Mazur, *Langmuir* **2009**, *25*, 1790–1794.

[5] P. P. Pompa, L. Martiradonna, A. Della Torre, F. Della Sala, L. Manna, M. De Vittorio, F. Calabi, R. Cingolani, R. Rinaldi, *Nat. Nanotechnol.* **2006**, *1*, 126–130.

[6] A. Pokhriyal, M. Lu, V. Chaudhery, C. S. Huang, S. Schulz, B. T. Cunningham, *Opt. Express* **2010**, *18*, 24793–24808.

[7] M. R. Gartia, J. P. Eichorst, R. M. Clegg, G. L. Liu, *Appl. Phys. Lett.* **2012**, 101.

[8] Y. Fu, J. Zhang, J. R. Lakowicz, *J. Fluoresc.* **2007**, *17*, 811.

[9] W. Zhang, N. Ganesh, P. C. Mathias, B. T. Cunningham, *Small* **2008**, *4*, 2199–2203.

[10] C. Graf, W. Schartl, K. Fischer, N. Hugenberg, M. Schmidt, *Langmuir* **1999**, *15*, 6170–6180.

[11] J. W. Gilliland, K. Yokoyama, W. T. Yip, *Chem. Mater.* **2005**, *17*, 6702–6712.

[12] M. Casalboni, R. Senesi, P. Prosposito, F. DeMatteis, R. Pizzoferrato, *Appl. Phys. Lett.* **1997**, *70*, 2969–2971.

[13] E. Herz, H. Ow, D. Bonner, A. Burns, U. Wiesner, *J. Mater. Chem.* **2009**, *19*, 6341–6347.

[14] H. Ow, D. R. Larson, M. Srivastava, B. A. Baird, W. W. Webb, U. Wiesner, *Nano Lett.* **2005**, *5*, 113–117.

[15] D. R. Larson, H. Ow, H. D. Vishwasrao, A. A. Heikal, U. Wiesner, W. W. Webb, *Chem. Mater.* **2008**, *20*, 2677–2684.

[16] D. L. Ma, A. J. Kell, S. Tan, Z. J. Jakubek, B. Simard, *J. Phys. Chem. C* **2009**, *113*, 15974–15981.

[17] D. Toptygin, R. S. Savtchenko, N. D. Meadow, S. Roseman, L. Brand, *J. Phys. Chem. B* **2002**, *106*, 3724–3734.

[18] D. Nguyen, D. Taylor, K. Qian, N. Norouzi, J. Rasmussen, S. Botzet, M. Lehmann, K. Halverson, M. Khine, *Lab Chip* **2010**, *10*, 1623–1626.

[19] C. C. Fu, A. Grimes, M. Long, C. G. L. Ferri, B. D. Rich, S. Ghosh, S. L. P. Lee, A. Gopinathan, M. Khine, *Adv. Mater.* **2009**, *21*, 4472.

[20] T. C. Lu, X. S. Chen, Q. Shi, Y. Wang, P. B. Zhang, X. B. Jing, *Acta Biomater.* **2008**, *4*, 1770–1777.

[21] G. Demirel, T. Caykara, B. Akaoglu, M. Cakmak, *Surf. Sci.* **2007**, *601*, 4563–4570.

[22] B. L. Zhang, S. Dallo, R. Peterson, S. Hussain, W. T. Tao, J. Y. Ye, *J. Biomed. Opt.* **2011**, 16.

[23] H. Bai, R. H. Wang, B. Hargis, H. G. Lu, Y. B. Li, *Sensors* **2012**, *12*, 12506–12518.

[24] E. P. Diamandis, T. K. Christopoulos, *Clin. Chem.* **1991**, *37*, 625–636.

[25] F. del Monte, J. D. Mackenzie, D. Levy, *Langmuir* **2000**, *16*, 7377–7382.

[26] J. Dakin, R. G. W. Brown, in *Handbook of Optoelectronics*, Taylor & Francis, New York **2006**.

[27] A. T. Young, *Appl. Optics* **1981**, *20*, 533–535.

[28] J. R. Lakowicz, in *Principles of Fluorescence Spectroscopy*, 3rd ed., Springer, New York **2006**.

[29] S. Link, M. A. El-Sayed, *Int. Rev. Phys. Chem.* **2000**, *19*, 409–453.

[30] D. Nawarathna, N. Norouzi, J. McLane, H. Sharma, N. Sharac, T. Grant, A. Chen, S. Strayer, R. Ragan, M. Khine, *Appl. Phys. Lett.* **2013**, 102.